

TITLE PAGE

Type of manuscript:

Full paper

Title:

Image guidance and inter-fractional anatomical variation in paediatric abdominal radiotherapy

Short title:

Image guidance for abdominal change in paediatric radiotherapy

Author list:

Sabrina Taylor[1], Pei Lim[2], Jessica Cantwell[3], Derek D'Souza[3], Syed Moinuddin[3], Yen-Ching Chang[2], Mark N. Gaze[2], Jennifer Gains[2], Catarina Veiga[1]

Affiliations:

[1]University College London, Centre for Medical Image Computing, London, United Kingdom

[2]University College London Hospitals NHS Foundation Trust, Department of Oncology, London, United Kingdom

[3]University College London Hospitals NHS Foundation Trust, Radiotherapy, London, United Kingdom

Corresponding author:

Dr Catarina Veiga

Centre for Medical Image Computing

Room 8.19, 8th Floor Malet Place Engineering Building

Malet Place, WC1E 6BT, London, United Kingdom

c.veiga@ucl.ac.uk; +44(0)7871912517

Acknowledgements:

This work was supported by the Radiation Research Unit at the Cancer Research UK City of London Centre Award [C7893/A28990]. Pei Lim was supported by the Children's Cancer and Leukaemia Group (CCLG) and the Little Princess Trust Grant award (CCLGA 2019 11). Mark Gaze was supported by the National Institute for Health Research Biomedical Research Centre of University College London Hospitals and by the Radiation Research Unit at the Cancer Research UK City of London Centre Award [C7893/A28990]. Jennifer Gains was supported by the Radiation Research Unit at the Cancer Research UK City of London Centre Award [C7893/A28990].) Catarina Veiga was supported by the Royal Academy of Engineering under the Research Fellowship scheme (RF\201718\17140).

This work was presented in part at the 53rd Annual Congress of the International Society for paediatric Oncology (SIOP), October 2021, online, and at the European Society for Radiotherapy and Oncology (ESTRO) 2022 Congress, May 2022, Copenhagen (Denmark).

ABSTRACT

Objectives: To identify variables predicting inter-fractional anatomical variations measured with cone-beam CT (CBCT) throughout abdominal paediatric radiotherapy, and to assess the potential of surface-guided radiotherapy (SGRT) to monitor these changes.

Methods: Metrics of variation in gastrointestinal (GI) gas volume and separation of the body contour and abdominal wall were calculated from 21 planning CTs and 77 weekly CBCTs for 21 abdominal neuroblastoma patients (median 4y, range: 2 –19y). Age, sex, feeding tubes, and general anaesthesia (GA) were explored as predictive variables for anatomical variation. Furthermore, GI gas variation was correlated with changes in body and abdominal wall separation, as well as simulated SGRT metrics of translational and rotational corrections between CT/CBCT.

Results: GI gas volumes varied 74±54 ml across all scans, while body and abdominal wall separation varied 2.0±0.7 mm and 4.1±1.5 mm from planning, respectively. Patients <3.5y (P=0.04) and treated under GA (P<0.01) experienced greater GI gas variation; GA was the strongest predictor in multivariate analysis (P<0.01). Absence of feeding tubes was linked to greater body contour variation (P=0.03). GI gas variation correlated with body (R=0.53) and abdominal wall (R=0.63) changes. The strongest correlations with SGRT metrics were found for anterior-posterior translation (R=0.65) and rotation of the left-right axis (R=-0.36).

Conclusions: Young age, GA, and absence of feeding tubes were linked to stronger inter-fractional anatomical variation and are likely indicative of patients benefiting from adaptive/robust planning pathways. Our data suggests a role for SGRT to inform the need for CBCT at each treatment fraction in this patient group.

Advances in knowledge: This is the first study to suggest the potential role of SGRT for the management of internal inter-fractional anatomical variation in paediatric abdominal radiotherapy.

1. Introduction

Neuroblastoma accounts for around 6% of all paediatric cancers in the United Kingdom, and radiotherapy plays a pivotal role in the multimodal treatment pathway for high-risk and some intermediate-risk patients [1–4]. Radiotherapy starts with the acquisition of a planning computed tomography (CT) scan for delineation of both target volumes and organs-at-risk, followed by dosimetric planning and treatment optimisation. The optimised radiotherapy plan is then delivered fractionated over several weeks of treatment. However, the planning CT represents a snapshot of the patient's anatomy at a specific point in time and the internal anatomy at each treatment fraction may vary due to day-to-day changes in organ filling, body weight, and tumour size, amongst other reasons [5,6]. Approximately 80% of neuroblastoma tumours are located within the abdomen [7], and this part of the body is susceptible to anatomical variations due to the highly variable lumen contents in the gastrointestinal (GI) tract [8]. This may compromise the conformality of the dose distributions delivered, leading to tumour underdosage (potentially resulting in increased risk of recurrence) or overdosage of normal tissues (potentially resulting in excessive toxicity) [8,9]. Accurate treatment delivery is particularly important for high-risk neuroblastoma patients given that the 5-year overall survival rate remains ~50% [4,10].

The growing use of highly conformal radiotherapy modalities aiming to improve outcomes in high-risk paediatric abdominal neuroblastoma, such as intensity modulated arc therapy (IMAT) and proton beam therapy (PBT) [9,11], make it increasingly important to monitor and account for anatomical change. PBT is an attractive treatment option for children due to its better tissue-sparing capabilities, but variations in the tissue density and composition may distort these desirable dose distributions. GI gas volume has been reported to vary as much as 80% during treatment compared to planning CT in pancreatic cancer radiotherapy plans [12] and this variation has been linked with proton dose degradation in cervical, gastric and pancreatic cancer patients [8,13–15]. Given that treatment pathways for adults differ greatly from children, there is a knowledge gap where findings on inter-fractional observations may not be accurately extrapolated to inform paediatric radiotherapy plans. Only a few studies have focused exclusively on inter-fractional variations in paediatric abdominal radiotherapy with assessment of bowel variation still being poorly investigated [16–18]. Lim et al reported that GI gas variation may compromise PBT dosimetry in children with high-risk midline neuroblastoma, reporting possible loss of the clinical target volume coverage up to 15.7% (compared to 1.9% for IMAT) [9]. Definite conclusions on the effect of anatomical variation on paediatric PBT dosimetry however are limited by the small sample sizes [9,19].

Image-guided radiotherapy (IGRT) technologies, such as cone-beam-CT (CBCT), can identify three-dimensional anatomical variations, which provides the opportunity to review the dosimetry and adapt the plan if needed (online or offline). However, CBCT is associated with dose exposures which are of concern in paediatric radiotherapy given the risk of young children developing radiation-induced second malignant neoplasms later in life [20–22]. Considering imaging exposure in children is particularly important in the era of volumetric IGRT [23]. Daily CBCT imaging doses are small (3 – 9 cGy and 9 – 29 cGy per CBCT scan for soft tissue and bones,

respectively, estimated on a 31-month abdominal paediatric phantom [24]) in comparison to the total therapeutic dose levels, but the cumulative dose of using daily CBCTs over all treatment fractions is of similar magnitude to the typical prescribed doses per fraction. For reference, currently radiotherapy is delivered in high-risk neuroblastoma in 1.5 – 1.8 Gy/fraction, up to approximately 21 Gy or 36 Gy (the latter being currently explored in on-going trials for patients with residual disease at the primary site after surgery) [25–27]. Surface-guided radiotherapy (SGRT) offers an attractive solution to complement current IGRT protocols by tracking the patient's skin surface. While SGRT has mostly been used to simplify patient set up protocols, there is a potential that surface images may also be able to detect internal anatomical variations and trigger adaptive radiotherapy pathways, although this potential has not yet been demonstrated in paediatric abdominal treatments [28–30].

A greater understanding of the degree and risks associated with abdominal anatomical changes during paediatric radiotherapy could inform optimal radiotherapy modality selection and the development of IGRT protocols and adaptive treatment pathways tailored to each abdominal neuroblastoma paediatric patient. Thus, this study aims to identify patient variables predicting inter-fractional anatomical variations for paediatric abdominal radiotherapy and to explore the potential of SGRT to detect and measure these changes. This study builds up from an exploratory analysis presented by XXXXX, where it was suggested that patient variables such as the use of general anaesthesia (GA) during radiotherapy may be associated with greater inter-fractional GI gas variation. Here we considerably expanded this preliminary analysis to include a larger dataset (n=21 vs n=11), and more comprehensively explore image-based metrics of inter-fractional variation (such as body and abdominal wall separation changes) and patient variables (such as the use of feeding tubes). To the best of our knowledge, this is the first study using volumetric imaging to quantify and to identify potential predictors inter-fractional anatomical change focusing on high-risk neuroblastoma paediatric patients, while exploring the novel use of SGRT technologies for its detection.

2. Materials and methods

This study included data from 21 paediatric patients with high-risk abdominal neuroblastoma historically treated with external beam radiotherapy. Patient characteristics are shown in Table 1. Patients did not receive concurrent chemotherapy. No dietary preparation was given prior to planning or treatment, and patients treated under GA received the same instructions for fasting for planning and treatment. The data for this study was requested and approved in line with the internal information governance procedures of the XXXXX Radiotherapy Department and provided anonymised.

2.1 Imaging scans and segmentations

All patients had one CT for treatment planning purposes and up to five weekly CBCTs acquired during treatment. A total of 21 CTs and 77 CBCTs were analysed and segmented for GI gas and body volumes. Segmentations were carried out semi-automatically using ITK-SNAP (Version 3.8.0) [31]. All contours were automatically post-processed to remove common manual segmentation errors. To define a common field-of-view between the two

modalities, CTs and CBCTs were rigidly co-registered using the open-source image registration algorithm NiftyReg [32].

2.2 Metrics

GI gas variation and weight changes are types of anatomical change frequently observed in the abdominal region. These variations were measured from CT and CBCT segmentations, as outlined in section 2.1, and converted to quantitative metrics as defined in Figure 1.

GI gas volumes were measured from the GI gas segmentations, from which we calculated the standard deviation of the GI volumes across all imaging timepoints (Gas_{std} [ml]), a measure of GI gas variability, as well as the absolute GI volume changes relative to the planning volumes (Gas_{rel} [ml]).

Changes to the body contour may be linked to both GI gas variation and weight loss. The abdominal wall adapts to the internal contents in the gut, such that abdominal distension is related to the volume of gas within the digestive tract [33]. Thus, we measured both variation in the whole-body contour and at the anterior surface of the body (surrogate for the abdominal wall) to decouple the effects of weight from GI changes. The closest distance between each voxel on the CT and CBCT body contour surface was calculated to generate a distance distribution (bi-directionally). The distributions were then used to calculate two complementary metrics: the signed and unsigned average distance ($Body_{avg}$ (signed) and $Body_{avg}$ (unsigned) [mm]). Unsigned distance metrics only measure the amount of the anatomical change, not the direction of the change – i.e., by how much the body contour has changed, but not if it shrank or expanded. Positive and negative (signed) distances allow visualisation of the relative position of the contours. For example, a negative signed $Body_{avg}$ (signed) indicates the CBCT is encompassed by the CT contour. To quantify changes at the abdominal wall, the signed/unsigned anterior-posterior distance between body contours at the anterior surface only was also calculated ($Surface_{avg}$ (signed) and $Surface_{avg}$(unsigned) [mm]).

Finally, surface correction metrics were calculated from the body contours to reflect the correction that a SGRT system would have obtained between planning and treatment position. The treatment position was simulated by applying a 6 degree-of-freedom transformation to align the CBCT with the CT (as described in section 2.1) followed by applying a translation to both scans such that their origins matched the radiotherapy treatment isocenter. The anterior surface was extracted from the body contours and converted to a set of points in space (point cloud). Point clouds were then registered using the iterative closest point algorithm in MATLAB 2019a (MathWorks Inc) to estimate the residual translational ($t_{x,y,z}$ [mm]) and rotational ($r_{x,y,z}$ [°]) corrections needed to align the CBCT surface to the reference (CT). This was done to investigate SGRT for inter-fractional anatomical monitoring, rather than set-up or intra-fractional motion monitoring.

2.3 Experimental design and statistical analysis

Two experiments were designed: (1) to identify variables predicting greater inter-fractional anatomical variations, and (2) to explore the correlation between volumetric and surface metrics of anatomical change. Sex, age, GA, and feeding tubes were explored as predictive variables for Gas_{std}, $Body_{avg}$ (unsigned) and $Surface_{avg}$ (unsigned). Age groups were defined by splitting the cohort into two: those aged <3.5 (n=8) and ≥3.5 (n=13) years. The volumetric and surface anatomical change metrics correlated are described in Figure 2. Statistical analyses were performed using Stata® MP Version 17.0 (StataCorp LLC) and Matlab 2019a. Statistical significance was assumed when P<0.05. A sensitivity analysis was conducted in all experiments by excluding the planning CT from the metrics calculation and, when applicable, defining as reference one of the CBCT scans randomly selected.

3. Results

3.1 Investigation of patient variables predictive of anatomical change

Gas_{std}, $Body_{avg}$ (unsigned) and $Surface_{avg}$ (unsigned) were on average 74±54 ml (range: 5 – 180 ml), 2.0±0.7mm (range: 0.9 – 3.6 mm) and 4.1±1.5 mm (range: 2.0 – 8.0 mm) throughout treatment across all patients. Patients exhibited on average a trend of reduction in GI gas, body contour and anterior surface across on all CBCT reviewed compared to planning (76%, 86%, and 90% of the patient group, respectively). GI gas variation seen throughout treatment is exemplified in Figure 2.

Gas_{std} was greater for subjects <3.5y (P=0.04) and under GA (P<0.01); $Body_{avg}$ (unsigned) was greater in patients without feeding tubes (P=0.03) (Figure 3). No variables predicted for $Surface_{avg}$ (unsigned). No additional variables predicted for Gas_{std} or $Body_{avg}$ (unsigned). All results are summarised in Table 2.

Statistically significant associations were established between (i) age and Gas_{std}, (ii) GA and Gas_{std}, and (iii) GA and age (Table 3). Multivariate linear regression analyses highlighted GA as the strongest driver for GI gas variation (P<0.01). Most patients aged <5.5y received treatment under GA (65%), whereas no patients aged ≥5.5y were anaesthetised. Only one patient aged <3.5y did not receive GA.

All findings remained valid when excluding the planning CT from analysis, only with the exception of the link between $Body_{avg}$ (unsigned) and feeding tubes (P=0.43) (Tables 2 and 3).

3.2 Correlations between volumetric and surface metrics of anatomical change

Gas_{rel}, was on average -86±138 ml (range: -468 – 262 ml). The signed separation of body contour ($Body_{avg}$ (signed)) and body surface ($Surface_{avg}$ (signed)) correlated moderately with Gas_{rel} (Figure 4), indicating a link between reduction in GI gas and shrinking of the body contours. Gas_{rel} was more strongly correlated with $Surface_{avg}$ (signed) (R=0.63) than with $Body_{avg}$ (signed) (R=0.53). Regarding metrics of surface correction, the strongest correlation with Gas_{rel} was found with anterior-posterior translation (t_y, R=0.65) and rotation of the left-right axis (r_x, R=-0.36). Similar correlations were found when excluding the planning CT from analysis. This

suggests that anterior surface changes were more likely affected by abdominal distension driven by GI gas variation, while body contour changes were more likely affected by other inter-fractional variations, such as weight fluctuation and setup errors. Figure 5 shows the distribution values for each surface correction metric and their linear regression with Gas_{rel}. The ranges of values for t_y (-2.8±3.3 mm, range: -10.2 – 8.4 mm) and r_x (1.4±1.9°, range: -3.1 – 7.4°) are larger than the accuracy reported for commercial surface imaging systems (0.2 mm/0.2°) [28].

4. Discussion

This study found that children receiving radiotherapy were more prone to inter-fractional anatomical variations if they were younger than 3.5 years old, were treated under GA, or were not using a feeding tube. These findings may contribute to inform the selection of the best treatment modality for each patient, such as selecting IMAT versus PBT, and to identify cases benefiting from robust planning pathways and more frequent image-guided protocols to minimise dosimetric inaccuracies. Incorporating SGRT as a key part of clinical IGRT protocols has great promise in childhood cancer radiotherapy where a culture of gentle IGRT is desirable, with benefits including lower radiation doses and simplified workflows regarding immobilisation and anaesthesia needs [23]. Clinical experience in abdominal paediatric treatments highlighted challenges in the use of SGRT for positioning due to changes in the abdominal wall caused by bloating or constipation [28]. The established correlation between GI gas and body contour opens doors to explore SGRT as a complementary imaging modality to monitor internal changes occurring throughout radiotherapy, with no exposure costs to the patient. This is an exciting application that goes beyond its current clinical use for setup [34]. To the best of our knowledge, this is the first time the potential of SGRT to monitor anatomical changes on treatment is proposed in paediatric radiotherapy settings.

PBT has great potential to treat children's abdominal cancers due to its highly precise delivery and potential for fewer side-effects [9,19,35]. Nonetheless, studies have already shown how dose delivery in PBT may be greatly affected by anatomical variations [8,9,15]. These challenges may be tackled at two key stages of the radiotherapy pathway: accounted for during treatment planning and/or adapted for during treatment delivery with IGRT information. The need to account for anatomical variations in highly conformal radiotherapy settings has meant that robust planning and evaluation of radiotherapy plans are essential to maintain their quality in the presence of anatomical change [36–38]. Applying advanced planning strategies in patients predisposed to GI gas variation may help overcome the current challenges in using PBT to treat large complex tumours; findings from a planning study favoured IMAT in high-risk midline neuroblastomas when using standard planning techniques [9]. IGRT strategies also help to overcome challenges caused by anatomical change by providing a method of monitoring the anatomy and triggering the need for treatment adaption accordingly. The development of adaptive radiotherapy workflows for PBT is an active area of research [39]. In our opinion, treatment adaptation strategies that may be promising to deal with the non-deformable anatomical changes within the abdomen include online selection of the best "plan of the day" from a library of plans (optimised for different GI tract contents) or online dose restauration/full re-optimisation techniques [40,41]. The observed correlation between internal GI gas volume and external surface variation metrics suggests there is value in exploring SGRT

as a complementary paediatric imaging modality, from which easy-to-measure body surface metrics could be calculated. SGRT is a novel non-ionising imaging technique with unmet harvested potential to support safer radiotherapy treatments [23,42]. While our findings need to be validated with clinical SGRT data, our study provides preliminary evidence of SGRT's role in identifying timepoints with considerable GI variations, which could be used clinically to trigger more complex adaptive radiotherapy workflows. The key idea is that while SGRT would not replace CBCT imaging, it could enable a fully personalised IGRT schedule for each patient and reduce volumetric imaging to only required fractions. This would help optimising the frequency of repeat CBCT for each patient, minimising the radiation burden associated, thereby making it a promising tool in paediatric IGRT protocols. We aim to explore this clinically by validating our findings with paired clinical SGRT and CBCT data in treatment position to develop a traffic light system, where SGRT is used as initial screen to trigger CBCT at each fraction.

This study expanded previous work from XXXXX who also noted statistically significant greater GI gas variations in anaesthetised neuroblastoma patients during radiotherapy (median 38.4%, range: 27.5 – 55.7%), compared to those without GA (11.5%, range: 7.9 – 17%). However, no correlation was established between GI gas variation and age, which contrasts results from our study where age <3.5y was highlighted as a predictive variable. Firstly, these differences in results can be explained by the fact that our present study has a larger sample size (n=21 vs n=11), which likely prevented dilution of statistically significant variables. Secondly, the presented study used a semi-automated segmentation technique, compared to an automated-only technique used in XXXXX, aiming to reduce segmentation inaccuracies in CBCTs in the presence of scattering artifacts. Lastly, our present study was more comprehensive by analysing additional variations throughout radiotherapy, including body and abdominal wall separation changes.

Similarly, our findings corroborate well with Guerreiro et al (2019) where a cohort of 20 abdominal cancer patients aged 1 to 8 years old (including 11 neuroblastoma patients) displayed average GI gas changes of 99.4±126.9 ml (range: -216.7 – 454.7 ml), and patient diameter changes of 0.5±0.4 cm (range: -1.2 – 2.0 cm) between daily CBCT and CT [19]. There are, however, some disparities between body contour metrics such that the data is not directly comparable; our study considered the three-dimensional separation between CT and CBCT body contours, whereas Guerreiro *et al* (2019) assessed the distance separation in the anterior-posterior direction between the internal target volume centre of mass and the patient's surface between CTs and CBCTs.

Patients without feeding tubes were observed to have greater body contour variations, which may highlight the role of feeding tubes in mitigating weight changes. The pathophysiological burdens of cancer and side-effects of prior aggressive therapies could explain why weight loss is commonly reported in neuroblastoma patients [43]. Feeding tubes are often used to manage weight loss in cancer patients [44], which may explain why our study observed smaller body contour variations in patients using feeding tubes. Berger et al (2017) observed that cervical cancer patients experienced weight changes between -3.1 and 1.2% throughout proton therapy, and body outline variations had a greater dosimetric impact than GI gas variations [8]. Therefore, the link between feeding tubes and body contour variation suggests that patients without feeding tubes should be monitored more regularly when delivering very conformal radiotherapy. However, these findings were not

statistically significant when excluding the planning CT from analysis so further data is required. This is likely because excluding the pre-radiotherapy timepoint effectively shortens the time intervals analysed and weight loss is likely to occur over several weeks.

This study also highlighted GA as the strongest predictor for GI gas variation. This observation could be linked to the anaesthetic agent typically used in children, propofol, which targets calcium channels to induce a relaxing effect on smooth muscles lining the GI tract, including the oesophageal sphincter. The relaxation of sphincters could be a possible route for air to enter the GI system and cause variable filling in patients repeatedly exposed to anaesthetic agents [45]. Air leaks are also a known side-effect of laryngeal mask airways used for GA patients since its distal end could interfere with the oesophageal sphincter and cause gastric insufflation [46]. Younger children are more likely to have radiotherapy under GA due to their limited compliance to lying still during radiotherapy compared to older children [47]. Given that younger children are the target audience for PBT, their reliance on GA could indicate they will be more susceptible to anatomical variations during treatment, thereby highlighting the need for robust treatment planning and evaluation techniques for these patients. The clinical implementation of SGRT brings the opportunity of increasing the safety of dose delivery in children allowing to stop treatment in real-time if movement is detected [28]. This may bring confidence to reduce the use of GA particularly in older, more compliant children.

This study has certain limitations. First, we simulated SGRT in treatment position based on CBCT information and a 6 degree-of-freedom couch. This will inherently result in alignments different from those that would be achieved using standard couches and/or setup workflows with skin marks and/or planar kV imaging. Therefore, our findings need to be validated with clinical SGRT data in treatment position. Furthermore, our sample size is considered small which risks dismissing statistically significant results. Visualisation of the bowel on CBCT is very limited so our analysis was restricted to GI gas content variation. Future studies using CT-on-rails or MRI for IGRT would be of interest to investigate if our findings would apply to more complex metrics of daily bowel displacement [48,49]. Manual editing of segmentations is prone to human errors, and the poor imaging quality of CBCTs and motion artifacts may compromise delineation accuracy. Other patient variables may be predictive of variations in contents of GI track – chemotherapy is also used in the treatment of high-risk neuroblastoma prior to radiotherapy [25] and may be associated with GI side-effects such as chemotherapy-induced enteritis and pneumatosis [50,51]. Moving forward, this study can inform future studies investigating methods of monitoring and accounting for anatomical changes during radiotherapy. We recommend larger sample sizes and analysis of additional patient variables, including weight monitoring and details on combination treatments used, as predictors of anatomical variation.

5. Conclusion

Patient variables, such as age, GA and absence of feeding tubes, were associated with greater inter-fractional anatomical variations. These factors may be useful to (1) inform on the selection of optimal radiotherapy modalities for each abdominal neuroblastoma patient, (2) help flag patients for robust planning and evaluation who are expected to be on a trajectory for greater inter-fractional anatomical variations and (3) select cases that

would benefit from frequent imaging monitoring. SGRT could be a valuable tool to assist the detection of anatomical changes during treatment delivery. The incorporation of SGRT in paediatric IGRT protocols may be useful to optimise the frequency of repeat CBCT for each patient, minimising imaging exposure.

Table and Figure Captions

Table 1. Patient characteristics.

Figure 1. Definition of the metrics of inter-fractional anatomical change and surface correction between planning computed tomography (CT) and cone-beam CT (CBCT).

Table 2. Statistical analysis for variables predicting anatomical change.

Table 3. Correlation coefficient between patient variables and gastrointestinal gas variation.

Figure 2. Example of variability in gastrointestinal gas and body contour between planning computed tomography (CT) and multiple weekly cone beam CT (CBCT) scans (Gas_{std}=171 ml for this subject).

Figure 3. Boxplots of gastrointestinal (GI) gas volume (Gas_{std}) variation according to age and general anaesthesia, and body contour variation ($Body_{avg}$) according to absence or presence of feeding tubes. Outliers represent values outside 1.5x the interquartile range.

Figure 4. Correlation between gastrointestinal gas variation (Gas_{rel}) and metrics of body change ($Body_{avg}$), abdominal wall change ($Surface_{avg}$) and surface correction metrics ($t_{x,y,z}$ and $r_{x,y,z}$). Gas_{rel}^{+} indicates the correlations when the CT scan was excluded from the analysis.

Figure 5. a) Distribution of values measured for surface correction metrics ($t_{x,y,z}$ and $r_{x,y,z}$) and b) linear regression with gastrointestinal gas variation (Gas_{rel})

References

[1] Public Health England. Children, teenagers and young adults UK cancer statistics report 2021. n.d.

[2] Colon NC, Chung DH. Neuroblastoma. Adv Pediatr 2011;58:297–311. https://doi.org/10.1016/j.yapd.2011.03.011.

[3] Arumugam S, Manning-Cork NJ, Gains JE, Boterberg T, Gaze MN. The Evidence for External Beam Radiotherapy in High-Risk Neuroblastoma of Childhood: A Systematic Review. Clin Oncol 2019;31:182–90. https://doi.org/10.1016/j.clon.2018.11.031.

[4] Tas ML, Reedijk AMJ, Karim-Kos HE, Kremer LCM, Ven CP van de, Dierselhuis MP, et al. Neuroblastoma between 1990 and 2014 in the Netherlands: Increased incidence and improved survival of high-risk neuroblastoma. Eur J Cancer 2020;124:47–55. https://doi.org/10.1016/j.ejca.2019.09.025.

[5] Sonke J-J, Aznar M, Rasch C. Adaptive Radiotherapy for Anatomical Changes. Semin Radiat Oncol 2019;29:245–57. https://doi.org/10.1016/j.semradonc.2019.02.007.

[6] Bertholet J, Anastasi G, Noble D, Bel A, Leeuwen R van, Roggen T, et al. Patterns of practice for adaptive and real-time radiation therapy (POP-ART RT) part II: Offline and online plan adaption for interfractional changes. Radiother Oncol 2020;153:88–96. https://doi.org/10.1016/j.radonc.2020.06.017.

[7] Sung KW, Yoo KH, Koo HH, Kim JY, Cho EJ, Seo YL, et al. Neuroblastoma Originating from Extra-abdominal Sites: Association with Favorable Clinical and Biological Features. J Korean Med Sci 2009;24:461–7. https://doi.org/10.3346/jkms.2009.24.3.461.

[8] Berger T, Petersen JBB, Lindegaard JC, Fokdal LU, Tanderup K. Impact of bowel gas and body outline variations on total accumulated dose with intensity-modulated proton therapy in locally advanced cervical cancer patients. Acta Oncol 2017;56:1472–8. https://doi.org/10.1080/0284186X.2017.1376753.

[9] Lim PS, Rompokos V, Bizzocchi N, Gillies C, Gosling A, Royle G, et al. Pencil Beam Scanning Proton Therapy Case Selection for Paediatric Abdominal Neuroblastoma: Effects of Tumour Location and Bowel Gas. Clin Oncol 2020;0. https://doi.org/10.1016/j.clon.2020.08.012.

[10] Matthay KK, Maris JM, Schleiermacher G, Nakagawara A, Mackall CL, Diller L, et al. Neuroblastoma. Nat Rev Dis Primer 2016;2:1–21. https://doi.org/10.1038/nrdp.2016.78.

[11] Gains JE et al. Intensity-modulated arc therapy to improve radiation dose delivery in the treatment of abdominal neuroblastoma. Future Oncol 2013;9:439–49.

[12] Estabrook NC, Corn JB, Ewing MM, Cardenes HR, Das IJ. Dosimetric impact of gastrointestinal air column in radiation treatment of pancreatic cancer. Br J Radiol 2018;91:20170512. https://doi.org/10.1259/bjr.20170512.

[13] Mondlane G, Gubanski M, Lind PA, Ureba A, Siegbahn A. Comparison of gastric-cancer radiotherapy performed with volumetric modulated arc therapy or single-field uniform-dose proton therapy. Acta Oncol 2017;56:832–8. https://doi.org/10.1080/0284186X.2017.1297536.

[14] Ashida R, Nakamura M, Yoshimura M, Mizowaki T. Impact of interfractional anatomical variation and setup correction methods on interfractional dose variation in IMPT and VMAT plans for pancreatic cancer patients: A planning study. J Appl Clin Med Phys 2020;21:49–59. https://doi.org/10.1002/acm2.12883.

[15] Narita Y, Kato T, Takemasa K, Sato H, Ikeda T, Harada T, et al. Dosimetric impact of simulated changes in large bowel content during proton therapy with simultaneous integrated boost for locally advanced pancreatic cancer. J Appl Clin Med Phys 2021;22:90–8. https://doi.org/10.1002/acm2.13429.

[16] Huijskens SC, van Dijk IWEM, Visser J, Balgobind BV, te Lindert D, Rasch CRN, et al. Abdominal organ position variation in children during image-guided radiotherapy. Radiat Oncol 2018;13:173. https://doi.org/10.1186/s13014-018-1108-9.

[17] Guerreiro F, Seravalli E, Janssens GO, van de Ven CP, van den Heuvel-Eibrink MM, Raaymakers BW. Intra- and inter-fraction uncertainties during IGRT for Wilms' tumor. Acta Oncol 2018;57:941–9. https://doi.org/10.1080/0284186X.2018.1438655.

[18] Meijer KM, van Dijk IWEM, Huijskens SC, Daams JG, Balgobind BV, Bel A. Pediatric radiotherapy for thoracic and abdominal targets: Organ motion, reported margin sizes, and delineation variations – A systematic review. Radiother Oncol 2022;173:134–45. https://doi.org/10.1016/j.radonc.2022.05.021.

[19] Guerreiro F, Zachiu C, Seravalli E, Ribeiro CO, Janssens GO, Ries M, et al. Evaluating the benefit of PBS vs. VMAT dose distributions in terms of dosimetric sparing and robustness against inter-fraction anatomical changes for pediatric abdominal tumors. Radiother Oncol 2019;138:158–65. https://doi.org/10.1016/j.radonc.2019.06.025.

[20] Armstrong GT, Liu Q, Yasui Y, Neglia JP, Leisenring W, Robison LL, et al. Late Mortality Among 5-Year Survivors of Childhood Cancer: A Summary From the Childhood Cancer Survivor Study. J Clin Oncol 2009;27:2328–38. https://doi.org/10.1200/JCO.2008.21.1425.

[21] Bhakta N, Liu Q, Ness KK, Baassiri M, Eissa H, Yeo F, et al. The Cumulative Burden of Surviving Childhood Cancer: An Initial Report from the St. Jude Lifetime Cohort Study. Lancet Lond Engl 2017;390:2569–82. https://doi.org/10.1016/S0140-6736(17)31610-0.

[22] Dzierma Y, Mikulla K, Richter P, Bell K, Melchior P, Nuesken F, et al. Imaging dose and secondary cancer risk in image-guided radiotherapy of pediatric patients. Radiat Oncol Lond Engl 2018;13:168. https://doi.org/10.1186/s13014-018-1109-8.

[23] Hess CB, Thompson HM, Benedict SH, Seibert JA, Wong K, Vaughan AT, et al. Exposure Risks Among Children Undergoing Radiation Therapy: Considerations in the Era of Image Guided Radiation Therapy. Int J Radiat Oncol 2016;94:978–92. https://doi.org/10.1016/j.ijrobp.2015.12.372.

[24] Ding GX, Coffey CW. Radiation Dose From Kilovoltage Cone Beam Computed Tomography in an Image-Guided Radiotherapy Procedure. Int J Radiat Oncol 2009;73:610–7. https://doi.org/10.1016/j.ijrobp.2008.10.006.

[25] Ladenstein R, Pötschger U, Pearson ADJ, Brock P, Luksch R, Castel V, et al. Busulfan and melphalan versus carboplatin, etoposide, and melphalan as high-dose chemotherapy for high-risk neuroblastoma (HR-NBL1/SIOPEN): an international, randomised, multi-arm, open-label, phase 3 trial. Lancet Oncol 2017;18:500–14. https://doi.org/10.1016/S1470-2045(17)30070-0.

[26] Gustave Roussy, Cancer Campus, Grand Paris. High-Risk Neuroblastoma Study 2 of SIOP-Europa-Neuroblastoma (SIOPEN) NCT04221035. clinicaltrials.gov; 2022.

[27] Gains J, Patel A, Mandeville H, Stacey C, Smyth G, Talbot J, et al. A randomised phase II trial of radiotherapy dose escalation, facilitated by intensity-modulated arc therapy techniques, in high-risk neuroblastoma. Int J Radiat Oncol Biol Phys 2022;114:1069. https://doi.org/10.1016/j.ijrobp.2022.09.029.

[28] Hoisak, Paxton, Waghorn, Pawlicki. Surface Guided Radiation Therapy. 1st edition. Taylor & Francis; 2020.

[29] Batista V, Meyer J, Kügele M, Al-Hallaq H. Clinical paradigms and challenges in surface guided radiation therapy: Where do we go from here? Radiother Oncol J Eur Soc Ther Radiol Oncol 2020;153:34–42. https://doi.org/10.1016/j.radonc.2020.09.041.

[30] Zhao B, Maquilan G, Jiang S, Schwartz DL. Minimal mask immobilization with optical surface guidance for head and neck radiotherapy. J Appl Clin Med Phys 2018;19:17–24. https://doi.org/10.1002/acm2.12211.

[31] Yushkevich PA, Piven J, Hazlett HC, Smith RG, Ho S, Gee JC, et al. User-guided 3D active contour segmentation of anatomical structures: significantly improved efficiency and reliability. NeuroImage 2006;31:1116–28. https://doi.org/10.1016/j.neuroimage.2006.01.015.

[32] Ourselin S, Roche A, Subsol G, Pennec X, Ayache N. Reconstructing a 3D structure from serial histological sections. Image Vis Comput 2001;19:25–31. https://doi.org/10.1016/S0262-8856(00)00052-4.

[33] Azpiroz F. Intestinal gas dynamics: mechanisms and clinical relevance. Gut 2005;54:893–5. https://doi.org/10.1136/gut.2004.048868.

[34] Olch AJ, Chlebik A, Wong K. Application of SGRT in Pediatric Patients: The CHLA Experience. Surf. Guid. Radiat. Ther., CRC Press; 2020.

[35] Taylor S, Lim P, Ahmad R, Alhadi A, Harris W, Rompokos V, et al. Risk of radiation-induced second malignant neoplasms from photon and proton radiotherapy in paediatric abdominal neuroblastoma. Phys Imaging Radiat Oncol 2021;19:45–52. https://doi.org/10.1016/j.phro.2021.06.003.

[36] van de Schoot AJAJ, de Boer P, Crama KF, Visser J, Stalpers LJA, Rasch CRN, et al. Dosimetric advantages of proton therapy compared with photon therapy using an adaptive strategy in cervical cancer. Acta Oncol Stockh Swed 2016;55:892–9. https://doi.org/10.3109/0284186X.2016.1139179.

[37] Cummings D, Tang S, Ichter W, Wang P, Sturgeon JD, Lee AK, et al. Four-dimensional Plan Optimization for the Treatment of Lung Tumors Using Pencil-beam Scanning Proton Radiotherapy. Cureus 2018;10:e3192. https://doi.org/10.7759/cureus.3192.

[38] Unkelbach J, Alber M, Bangert M, Bokrantz R, Chan TCY, Deasy JO, et al. Robust radiotherapy planning. Phys Med Biol 2018;63:22TR02. https://doi.org/10.1088/1361-6560/aae659.

[39] Albertini F, Matter M, Nenoff L, Zhang Y, Lomax A. Online daily adaptive proton therapy. Br J Radiol 2020;93:20190594. https://doi.org/10.1259/bjr.20190594.

[40] Borderías Villarroel E, Geets X, Sterpin E. Online adaptive dose restoration in intensity modulated proton therapy of lung cancer to account for inter-fractional density changes. Phys Imaging Radiat Oncol 2020;15:30–7. https://doi.org/10.1016/j.phro.2020.06.004.

[41] Bleeker M, Goudschaal K, Bel A, Sonke J-J, Hulshof MCCM, van der Horst A. Feasibility of cone beam CT-guided library of plans strategy in pre-operative gastric cancer radiotherapy. Radiother Oncol J Eur Soc Ther Radiol Oncol 2020;149:49–54. https://doi.org/10.1016/j.radonc.2020.04.057.

[42] Padilla L, Havnen-Smith A, Cerviño L, Al-Hallaq HA. A survey of surface imaging use in radiation oncology in the United States. J Appl Clin Med Phys 2019;20:70–7. https://doi.org/10.1002/acm2.12762.

[43] Mahapatra S, Challagundla KB. Neuroblastoma. StatPearls, Treasure Island (FL): StatPearls Publishing; 2022.

[44] Wiggenraad RGJ, Flierman L, Goossens A, Brand R, Verschuur HP, Croll GA, et al. Prophylactic gastrostomy placement and early tube feeding may limit loss of weight during chemoradiotherapy for advanced head and neck cancer, a preliminary study. Clin Otolaryngol Off J ENT-UK Off J Neth Soc Oto-Rhino-Laryngol Cervico-Facial Surg 2007;32:384–90. https://doi.org/10.1111/j.1749-4486.2007.01533.x.

[45] Tran K, Kuo B, Zibaitis A, Bhattacharya S, Cote C, Belkind-Gerson J. Effect of propofol on anal sphincter pressure during anorectal manometry. J Pediatr Gastroenterol Nutr 2014;58:495–7. https://doi.org/10.1097/MPG.0000000000000190.

[46] Ho-Tai LM, Devitt JH, Noel AG, O'Donnell MP. Gas leak and gastric insufflation during controlled ventilation: face mask versus laryngeal mask airway. Can J Anaesth J Can Anesth 1998;45:206–11. https://doi.org/10.1007/BF03012903.

[47] Stackhouse C. The use of general anaesthesia in paediatric radiotherapy. Radiography 2013;19:302–5. https://doi.org/10.1016/j.radi.2013.08.004.

[48] Nonaka H, Onishi H, Watanabe M, Nam VH. Assessment of abdominal organ motion using cine magnetic resonance imaging in different gastric motilities: a comparison between fasting and postprandial states. J Radiat Res (Tokyo) 2019;60:837–43. https://doi.org/10.1093/jrr/rrz054.

[49] Li S, Gong Y, Yang Y, Guo Q, Qian J, Tian Y. Evaluation of small bowel motion and feasibility of using the peritoneal space to replace bowel loops for dose constraints during intensity-modulated radiotherapy for rectal cancer. Radiat Oncol 2020;15:211. https://doi.org/10.1186/s13014-020-01650-z.

[50] Viswanathan C, Bhosale P, Moorthy Ganeshan D, Truong MT, Silverman P, Balachandran A. Imaging of complications of oncological therapy in the gastrointestinal system. Cancer Imaging 2012;12:163–72. https://doi.org/10.1102/1470-7330.2012.0014.

[51] McQuade RM, Stojanovska V, Abalo R, Bornstein JC, Nurgali K. Chemotherapy-Induced Constipation and Diarrhea: Pathophysiology, Current and Emerging Treatments. Front Pharmacol 2016;7:414. https://doi.org/10.3389/fphar.2016.00414.

Fig 1 Metric	Symbol	Definition	Illustration
Variation in gastrointestinal (GI) gas	**Gas_{std}**	Standard deviation of GI gas volume over all scans (CT and CBCT)	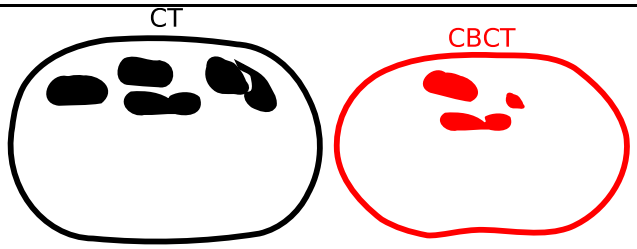
	Gas_{rel}	Absolute change in GI gas volume at CBCT, relative to CT [mL].	• Gas_{rel} <0 indicates smaller gas volumes at CBCT.
Variation in body contour separation	**$Body_{avg}$**	Average separation between CT and CBCT body contour over all scans [mm]. Distances were calculated both signed and unsigned to report two complementary metrics: • $Body_{avg}$ (signed) • $Body_{avg}$ (unsigned)	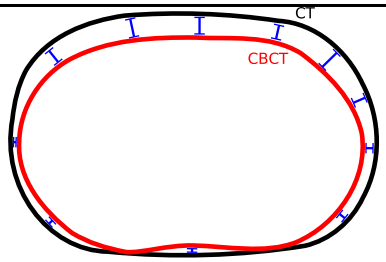 • $Body_{avg}$ (signed)<0 means the CBCT is encompassed by the pCT contour. $Body_{avg}$ (signed)>0 means the CBCT is surrounding the pCT contour. • $Body_{avg}$ (unsigned) is always >0, irrespective of one contour encompassing the other.
Variation in abdominal wall separation	**$Surface_{avg}$**	Average anterior-posterior separation between CT and CBCT body anterior surface [mm]. Distances were calculated both signed and unsigned to report two complementary metrics: • $Surface_{avg}$ (signed) • $Surface_{avg}$ (unsigned)	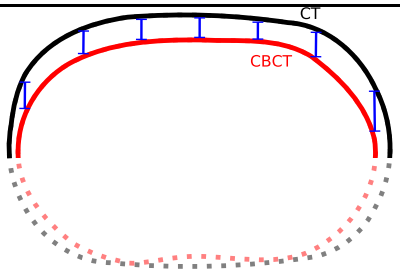 • $Surface_{avg}$ (signed)<0 means the CBCT is encompassed by the pCT contour. $Surface_{avg}$ (signed)>0 means the CBCT is surrounding the pCT contour. • $Surface_{avg}$ (unsigned) is always >0, irrespective of one contour encompassing the other.
Surface correction – translation	$t_{x,y,z}$	Translation matrix coefficients to align CBCT anterior surface to reference (pCT) [mm].	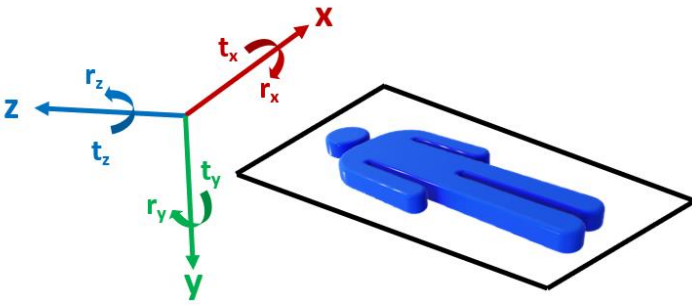
Surface correction – rotation	$r_{x,y,z}$	Rotation matrix coefficients to align CBCT anterior surface to reference (CT) [°].	

Fig 2

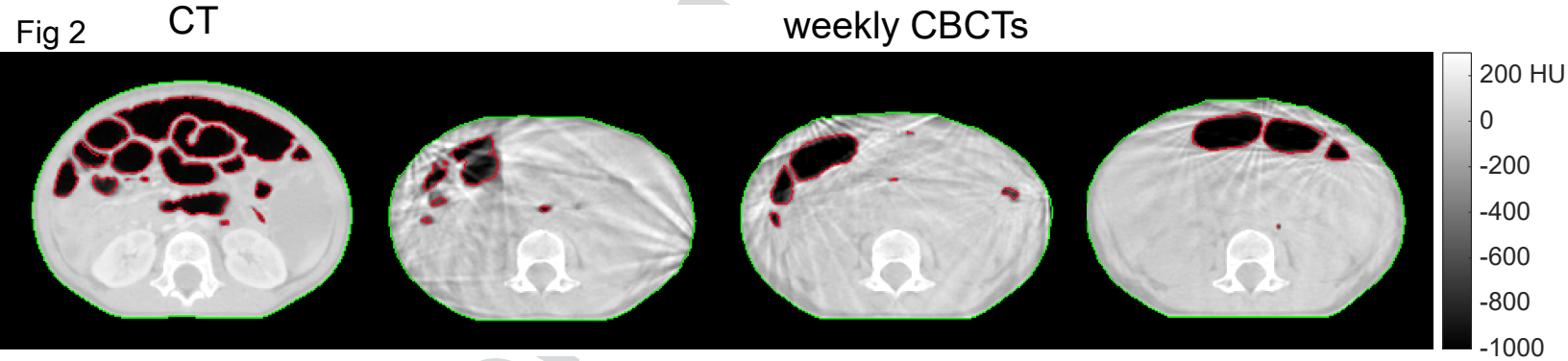

Fig 3

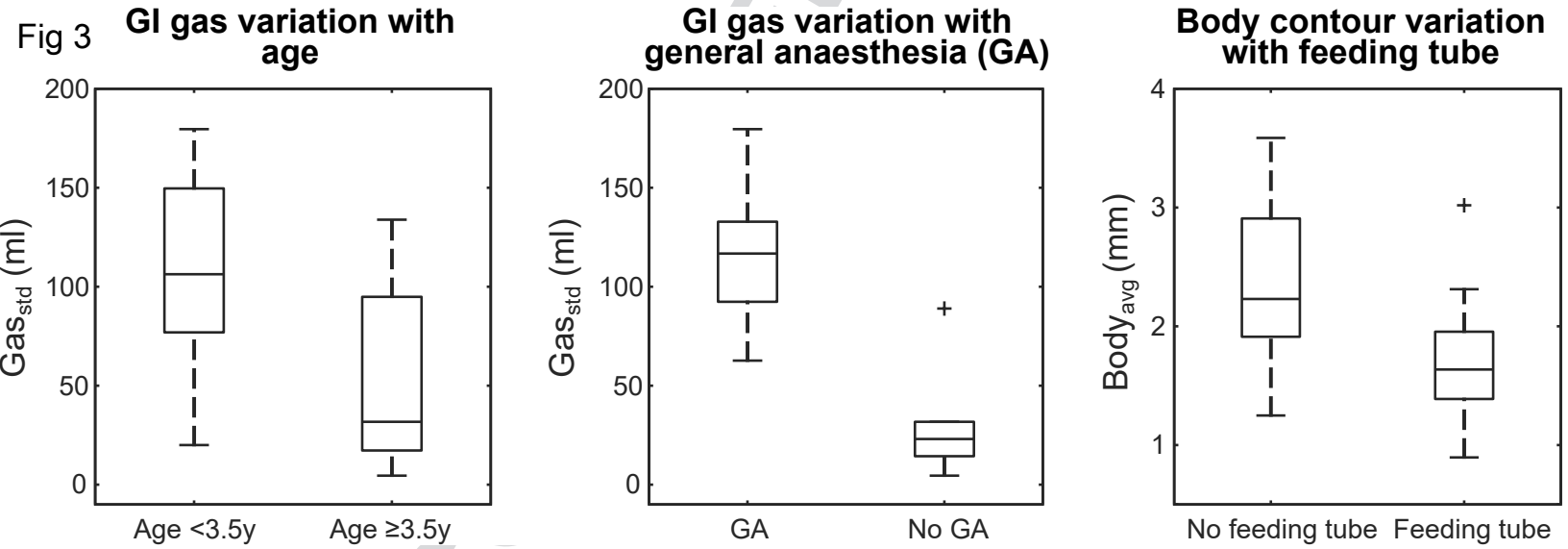

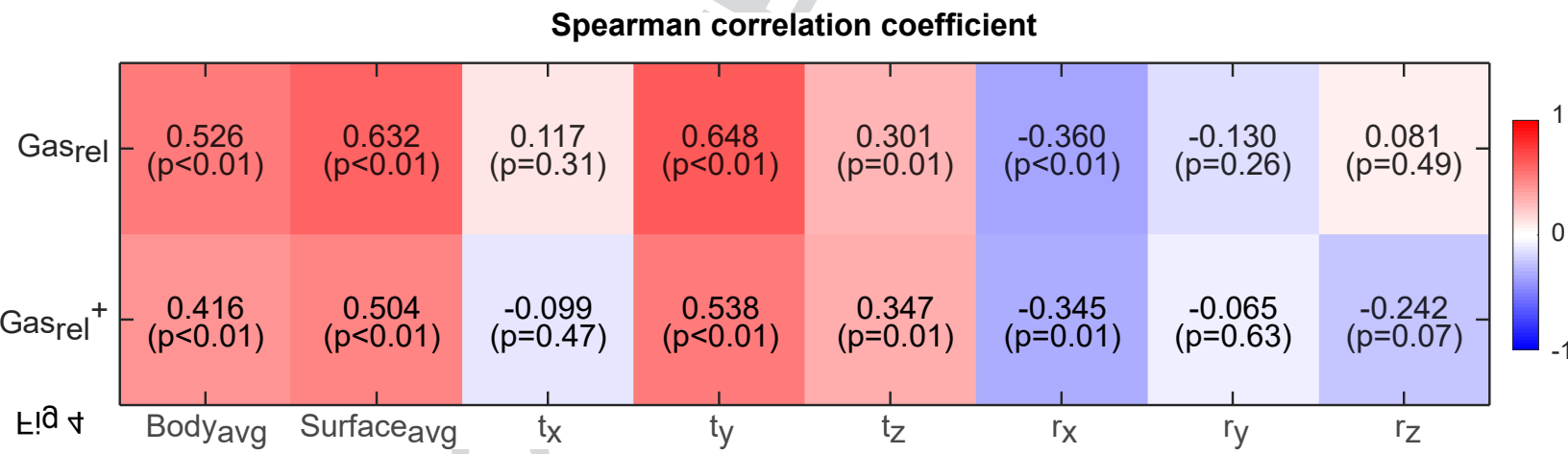

Fig 5

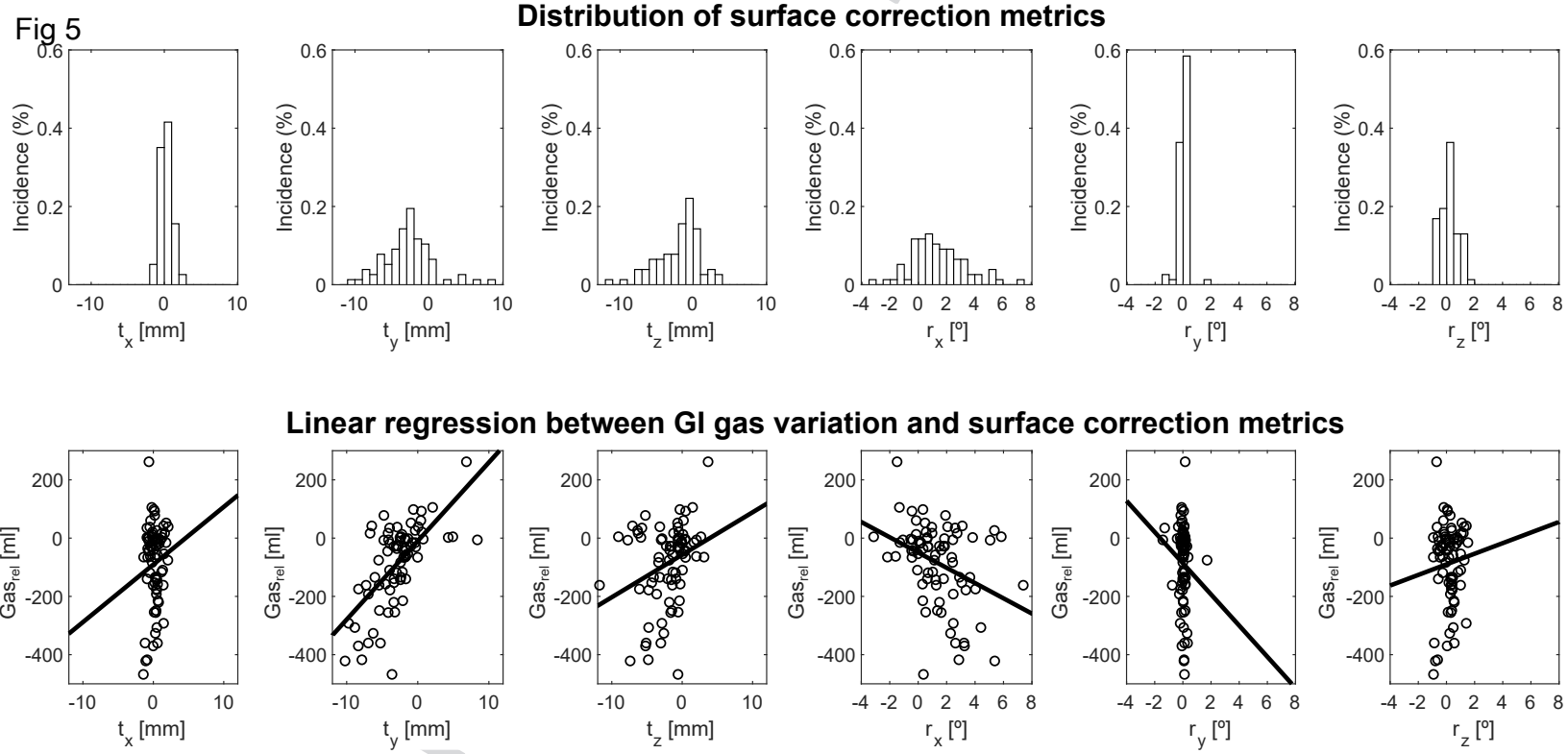

Table 1. Patient characteristics.

Patient characteristics	N=21
Age (years)	
Median	4
Mean (Range)	5 (2 – 19)
Ratio (%)	
Male : Female	10 : 11
General anaesthesia (GA) : No GA	11 : 10
Feeding tube : No feeding tube	12 : 9
Nasogastric tube : Percutaneous endoscopic gastrostomy	9 : 3

Table 2. Statistical analysis for variables predicting anatomical change.

Variables	P-value Mann-Whitney two-sample test		
	Gas_{std}	**$Body_{avg}$ (unsigned)**	**$Surface_{avg}$ (unsigned)**
Sex	0.439 (0.622)+	0.526 (0.622)+	0.526 (0.622)+
Age	0.043** (0.014**)+	0.717 (0.612)+	0.717 (0.828)+
General anaesthesia	<0.001*** (<0.001***)+	0.231 (0.159)+	0.573 (0.260)+
Feeding tube	0.155 (0.201)+	0.033** (0.434)+	0.055 (0.356)+

** P<0.05, *** P<0.01

+ indicates results when excluding the planning CT scan from the analysis

Table 3. Correlation coefficient between patient variables and gastrointestinal gas variation.

Variables	Correlation coefficient	P value
Age and Gas_{std}	R^a = -0.573 (-0.683)$^+$	0.007*** (<0.001***)$^+$
General Anaesthesia and Gas_{std}	$Coef^b$ = 0.069 (0.225)$^+$	<0.001*** (<0.001***)$^+$
General Anaesthesia and age	$Coef^b$ = -1.411	0.001***

** P<0.05, *** P<0.01

[a]R, Spearman's rank correlation test coefficient

[b]Coef, exact logistic regression coefficient

$^+$ indicates results when excluding the planning CT scan from the analysis